JOURNAL OF SPACECRAFT AND ROCKETS
Vol. 35, No. 3, May–June 1998

Aerodynamic Performance of Supersonic Missile Body- and Wing Tip-Mounted Lateral Jets

B. Srivastava*
Raytheon Electronics Systems, Tewksbury, Massachusetts 01876

Forward, missile body-mounted, lateral jet thrusters in a windward orientation yield amplification factors that are well below unity (∼0.5). This deamplification is caused by the intense interaction between the oncoming freestream and the jet flow, causing massive loss of the favorable pressure on the windward wings. Additionally, the jet flow creates a blockage effect that extends to the windward rear tail panels causing reduced tail control for this missile orientation. A means to enhance the amplification factor and regain control of tail panels is addressed by studying several alternate locations of the lateral jet thruster with a fixed body/wing/tail missile geometry. It is shown that the jet thrusters mounted on the wing tips enhance the amplification factor to 1.06 as compared to 0.5 for the forward missile body-mounted lateral thruster. This approach also recovers the control power of the windward rear tail panels. Specific generic missile studies are presented after extensive jet interaction validations of the computational method with the wind-tunnel data.

Nomenclature

AF	= amplification factor, $1 + (CN_{\text{jet}} - CN_{\text{no-jet}})/(T/q \cdot S)$
Clm	= rolling moment coefficient, $Mx/(q \cdot S \cdot X_{\text{ref}})$
Cm	= pitching moment coefficient, $My/(q \cdot S \cdot X_{\text{ref}})$
CN	= normal force coefficient, $(N/q \cdot S)$, airframe only
CY	= side force coefficient, $FY/(q \cdot S)$
CYm	= yawing moment coefficient, $Mz/(q \cdot S \cdot X_{\text{ref}})$
dp	= pressure differential, $(P_{\text{jet}} - P_{\text{no-jet}})/(\gamma \cdot P_{\text{inf}})$
FY	= side force, N
M	= freestream Mach number
Mx	= rolling moment
My	= pitching moment
Mz	= yawing moment
N	= normal force, N
P	= pressure, N/m^2
q	= dynamic pressure, $\frac{1}{2}\rho v^2$
S	= missile cross-sectional area, m^2
T	= jet thrust, N
v	= velocity, m/s
α	= angle of attack, deg
γ	= ratio of specific heats
ρ	= density
ϕ	= azimuth angle, deg

Subscripts

inf	= freestream condition
jet	= condition with jet (excluding jet thrust coefficient)
no-jet	= condition with no jet
X_{ref}	= reference length for normalization

Introduction

THE lateral jet control of a missile offers an attractive alternative to the conventional surface control for improved missile agility and maneuverability. The primary drivers for this are rapid missile response time and ability to perform at low speeds and high altitudes where dynamic pressures are low. A successful design effort based on the lateral jet controls, however, must develop a rational design basis for such factors as the jet size, locations, number of jets, thrust levels, effect of jet temperature, jet angle, and most importantly its interaction with the missile external flow. The problem of jet interaction with the external flow, under conditions of varying flight Mach numbers and angles of attack, is extremely complex in nature, and an understanding of this interaction is important to achieve optimal missile performance. A large volume of experimental and analytical studies related to lateral jets dating back to the 1960s is currently available in the literature.[1,2] However, despite these studies, numerous related issues need to be addressed.

Because of the complexity of the flow involved in this interaction process, a viable approach to address some of these issues is to judiciously combine wind-tunnel testing and computational fluid dynamics (CFD) simulations to evolve a validated design and analysis tool. The former provides a valuable database for CFD validation, whereas the latter provides a means for parametric design evaluation. This approach also offers a methodology to synthesize the physical complexity of the flow to identify key controlling parameters. This can be done by sequentially increasing the physical complexity of the model in a CFD simulation. At Raytheon, the design team has adopted this approach, i.e., scaled model testing, CFD validation, and design tradeoff studies using the validated CFD tools.

Numerous wind-tunnel and CFD studies[3–5] conducted in the past have demonstrated that a windward-oriented jet thruster yields amplification factors that are well below unity, i.e., deamplification of the thrust occurs due to the intense interaction between the freestream and the jet flow. The primary source of this deamplification is the massive loss of favorable pressure on the windward airframe components that fall in the shadow region of the jet (blockage effect). Additionally, the same shadow effect also extends to the windward rear tail panels, causing loss of tail control power. A small region of high positive pressure ahead of the jet provides the only mechanism to recover the loss of the normal force on the aft windward components. For a typical winged missile configuration, current studies suggest that it may be difficult to recover the loss of normal forces on the windward wings by attempting to increase the size of the positive pressure zone ahead of the thruster jet for a forward body-mounted jet thruster.[3] This paper explores the possibility of mounting thruster jets at alternate locations on the missile surface to achieve the following goals: 1) increase the thrust amplification factor to one or greater, 2) retain control power of the tail panels, and 3) minimize geometry changes from the baseline aerodynamic shape.

The next section briefly outlines the previous work in this area using CFD approaches. The details of the computational methodology, geometry, grid-related issues, and boundary conditions of the CFD applications are discussed later. A previous paper presented a large number of validation cases with the wind-tunnel data, with and without divert thrusters.[4] Further validation cases at a nominal Mach

Presented as Paper 97-2247 at the AIAA 15th Applied Aerodynamics Conference, Atlanta, GA, June 23–25, 1997; received July 11, 1997; revision received Nov. 7, 1997; accepted for publication Nov. 12, 1997.

*Senior Development Engineer, System Design Laboratory. Senior Member AIAA.

number of 4.0 and an angle of attack of 20 deg for an asymmetric missile configuration are discussed in the subsequent section. The bulk of the technical discussion related to the effect of divert thruster location on the missile performance is discussed in the section after that. The last section presents the summary and conclusions based on these computational studies.

Background

The topic of jet interaction with an external supersonic flow dates back to the mid-1960, when a large number of generic experimental data were generated and related correlation techniques were developed.[1,2] The emergence of hypersonic interceptors, maturity of CFD, and advent of supercomputers revived these activities in the late 1980s.[5–9] Several investigators have performed CFD studies for the fundamental problem of jet interaction in relation to adaptive gridding,[10] turbulence models,[11] grid refinements,[12] and the impact of artificial viscosity.[10] These studies range from Euler[13] to Navier–Stokes[14] computations. Of these studies, particular reference is made to the studies reported by Dash et al.[14] and York et al.[8] because much of the current CFD effort is derived from their mature technical expertise in this area. Further details of the methodology and related research work can be obtained from the references cited.

Although a vast number of numerical studies have been performed using controlled jet interaction studies for methodology development, efforts to simulate missile surfaces have been rather limited. Recently, Chan et al.[15] performed a series of studies that led to the simulation of a full missile surface with control surfaces and jet interaction. Qin and Foster[16] performed similar studies using a Navier–Stokes approach for an inclined jet on an ogive/cylinder body. These results depict the remarkable flow details obtained using CFD approaches, which ultimately result in making judicious choices for flight vehicle design and further wind-tunnel testing. Srivastava[3] performed full Navier–Stokes (FNS) studies for generic missile bodies with/without leeward and windward jets but without wing or tail panels. Comparisons with the wind-tunnel data, however, were not direct because the tests were conducted with tail panels, whereas computations were performed without tail. Removal of the tail load from the wind-tunnel data by an approximate method introduced uncertainties that were not fully quantified. This deficiency in the CFD model was eliminated later by Srivastava,[4] showing direct comparison of the CFD predictions with the wind-tunnel data by modeling all geometrical aspects of the wind-tunnel missile geometry and the divert thruster.

Computational Methodology

PARCH,[8] which is an FNS code with plume/missile airframe steady flow predictive capability, is being used for our current studies. PARCH utilizes formulations based on the NASA Ames Research Center ARC aerodynamic code and the Arnold Engineering Development Center propulsive extension, PARC. This code is particularly suited for missile surfaces due to its grid patching capability, which is useful for treating embedded surfaces in a flowfield. Patching, which is accomplished in mapped computational coordinates, is automatically constructed from boundary inputs. Boundary conditions are applied along the outer computational boundaries and relevant embedded surfaces. The code utilizes diagonalized Beam–Warming numerics with matrix-split finite rate chemistry. Several versions of the k–ϵ turbulence model are available in the code that were specifically developed for jet interaction and propulsive studies. We are using the capped low-Reynolds-number formulation of Chien's k–ϵ model[14] for the current simulations. Further details of the code capability can be found in Ref. 8.

Typical boundary approaches for the current application (supersonic flows) are specified supersonic freestream conditions at the inlet and outer boundaries. Extrapolation procedures are employed at the exit boundary. Surface conditions are appropriate to viscous flows with the adiabatic wall condition.

The surface jet boundary condition is the specified jet nozzle supersonic exit condition. The circular area of the jet in the wind-tunnel test is approximated by a square aperture in the CFD simulation.

Figure 1 shows a generic missile geometry. The wing in Fig. 1 is the baseline configuration, which is 6.3 body diameters long, and

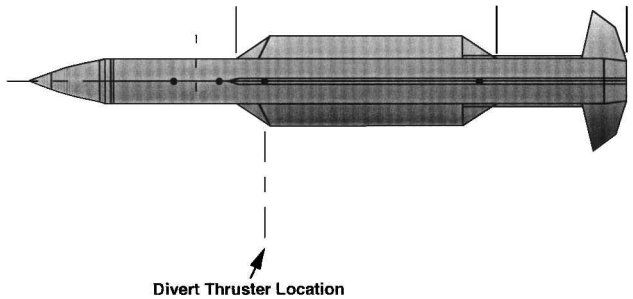

Fig. 1 Missile wind-tunnel test geometry.

its leading edge starts at 4.85 body diameters from the missile nose. The jet thruster is located at 5.6 body diameters from the nose. For all of the studies, this basic geometry remained the same; only the jet location was varied. CFD studies were conducted by moving the jet location from the forward part of the missile body (a nominal case) to the rear part of the missile body. For the latter case, the jet area and the total thrust were held fixed to the nominal case. Two variations of the wing tip-mounted jets were studied. In the first study, the wing shape was maintained to be the same as the nominal case and an equivalent rectangular slit on the wing-tips was used as the divert jet nozzle. To preserve the total thrust, this meant utilizing both windward wing tips, yielding a symmetric flow configuration. For both the forward- and rear-mounted wing tip divert jets, this arrangement yielded a narrow rectangular slit while maintaining the wing shape. In many respects, this is an idealized CFD study because structural integrity and packaging issues will dictate thicker wing near the divert jet location. This led us to study a more practical geometry for the wing shape, i.e., thick leading or trailing edge to accommodate the divert jet area, which tapers to the original thickness of the wing. For all of these cases, the total divert thrust level was maintained in the range of 180–216 lb, or thrust ratio of 3.5–4.25. For a plus orientation missile, only one wing tip is used, and therefore, the total thrust ratio is nearly 1.75 (half the stated value).

CFD simulations were performed on several different grids, which varied with the location of the lateral jet thruster. The overall distribution of the grid was modified to fit the jet thruster at various locations by keeping the total number of grid points constant for all cases, i.e., $230 \times 51 \times 69$. This grid was arrived at by performing a grid accuracy study. A grid patching procedure was used to apply the relevant boundary conditions on the surfaces. All angles of attack for a given configuration were simulated on a single grid, consistent with the minimum desired Mach number and maximum desired angle of attack. This method allows us to minimize the grid effort. The grids were generated through GRIDGEN, with geometry models developed within GRIDGEN.[17]

Current studies were performed for a nominal flow Mach number of 4 with an angle of attack of 20 deg with windward jet orientations, which encompasses the most severe flow case. This case also allows us to exploit symmetry in the CFD simulation to reduce computer time for each run.

Comparison with Wind-Tunnel Tests

In Refs. 3 and 4, numerous comparisons of the CFD predictions with the wind-tunnel data were made at a nominal Mach number of 4, angles of attack ranging from 2 to 25 deg, and leeward and windward jets with thrust ratios of 2 and 4 for a symmetric missile configuration. The results showed excellent comparisons of the CFD predictions with the wind-tunnel data. Further comparative studies are reported here, showing comparative results at the nominal Mach number of 4 for an asymmetric geometry at 20-deg angle of attack. Only brief discussions on these cases are provided for completeness.

Figure 2 shows a computation for a missile with four wing and tail panels at a flow Mach number of 3.94, an angle of attack of 20 deg, and an azimuthal angle of 109.42 deg (as shown in the inset of Fig. 2). This is a case without any divert thruster jet. Notice from Fig. 2 that the comparisons of the computational results with the wind-tunnel data are excellent for all force and moment coefficients. Three additional cases are presented to show the divert thruster effects on the flowfield. Figure 3 shows a computational result for a

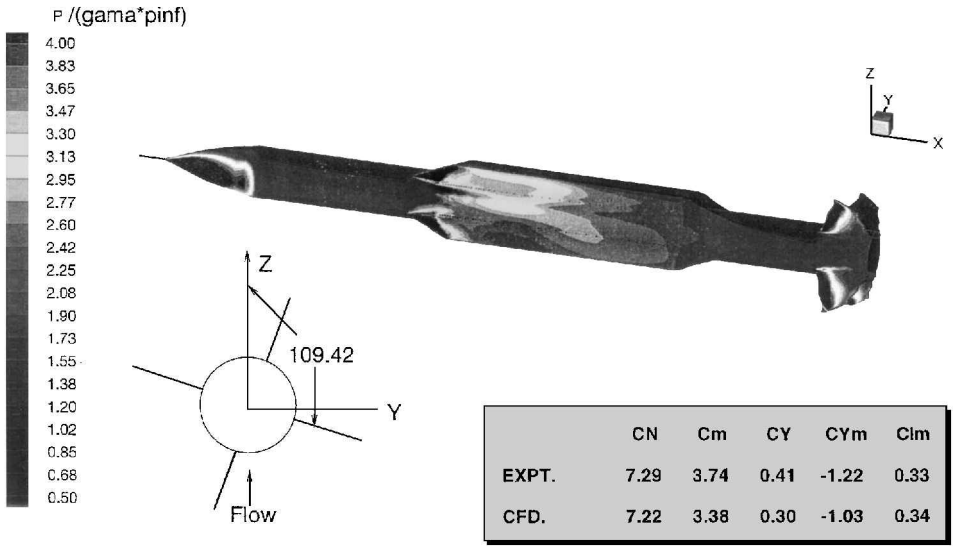

	CN	Cm	CY	CYm	Clm
EXPT.	7.29	3.74	0.41	-1.22	0.33
CFD.	7.22	3.38	0.30	-1.03	0.34

Fig. 2 CFD simulation of a supersonic asymmetric missile. Flow conditions: $M = 3.94$, $\alpha = 20$ deg, and $\phi = 109.42$ deg (no-jet case).

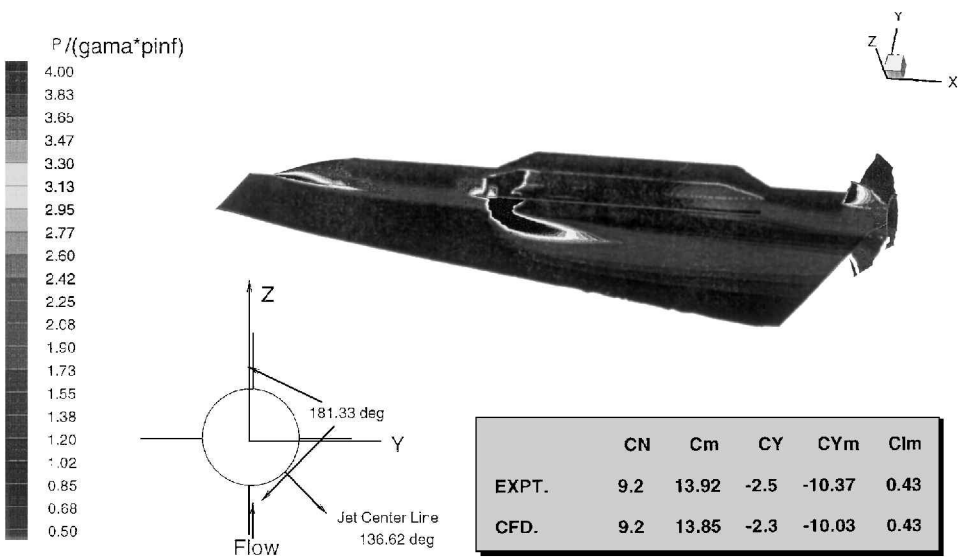

	CN	Cm	CY	CYm	Clm
EXPT.	9.2	13.92	-2.5	-10.37	0.43
CFD.	9.2	13.85	-2.3	-10.03	0.43

Fig. 3 Pressure distribution on jet center plane and missile surfaces for a windward jet. Flow conditions: $M = 3.94$, $\alpha = 20$ deg, $\phi = 181.33$ deg, and jet thrust = 175 lb.

forward missile body-mounted (see Fig. 1) windward side thruster with the thrust value of approximately 175 lb. Figure 3 shows the pressure distribution on the missile body and control surfaces and on a plane containing the windward jet. Remarkable jet interaction effects showing contours as well as excellent force and moment comparisons with the data are obvious from Fig. 3. Similar results are shown in Figs. 4 and 5, where divert thruster was rolled to the side orientation (Fig. 4) and to the leeward side (Fig. 5). In both of these computations, the predicted results compare remarkably well with the wind-tunnel data.

Results and Discussion

Validation results, as just outlined, allow one to proceed with the design tradeoff studies with some confidence. The discussions presented next address means to improve the divert thruster performance, specifically for the windward jet orientation.

Missile Body-Mounted Jet Thruster

Forward Jet

Figure 6 shows the computed surface pressure contours for two cases. The top of Fig. 6 is with a forward missile body-mounted windward jet, jet thrust coefficient (defined as jet thrust/$q \cdot S$, where q is the dynamic head and S is the missile body cross-sectional area) of 3.45, at a flow Mach number of 3.94, and at angle of attack of 20 deg. The missile is in X orientation with interdigitated divert thruster. For this case, notice the extent of high pressure forward of the jet and very low pressures aft of the jet on the windward side. It is quite clear from Fig. 6 that the presence of the jet on the surface has totally wiped out the normal forces created by the windward wings. This is clearer if we compare the lower part of Fig. 6, which shows jet-off pressure contours, with the upper jet-on part. The inset table of Fig. 6 shows the comparison of the normal force and pitching moment coefficients with the wind-tunnel data. The comparisons are excellent. Overall we can conclude the following from Fig. 6.

1) A windward-located jet thruster creates a favorable high-pressure zone ahead of the jet, only at the expense of massive loss of normal force from the windward wings.

2) For this case the thrust amplification factor (defined as 1+ aerointeractive force/thrust) is 0.48. Note, however, that the pitching moment is significantly increased with the jet thrusters. Even though the latter can be used effectively to our advantage for vehicle maneuver, our goal is to also enhance the amplification factor.

3) Note also from Fig. 6 that a jet wraparound effect is seen to create an adverse effect causing undesirable normal forces.

4) The effect of the jet gas on the tail panels is massive, resulting in total loss of control power for this jet orientation.

These effects were observed in previous computations,[3] but now the results are far more credible due to the excellent comparisons with wind-tunnel data.

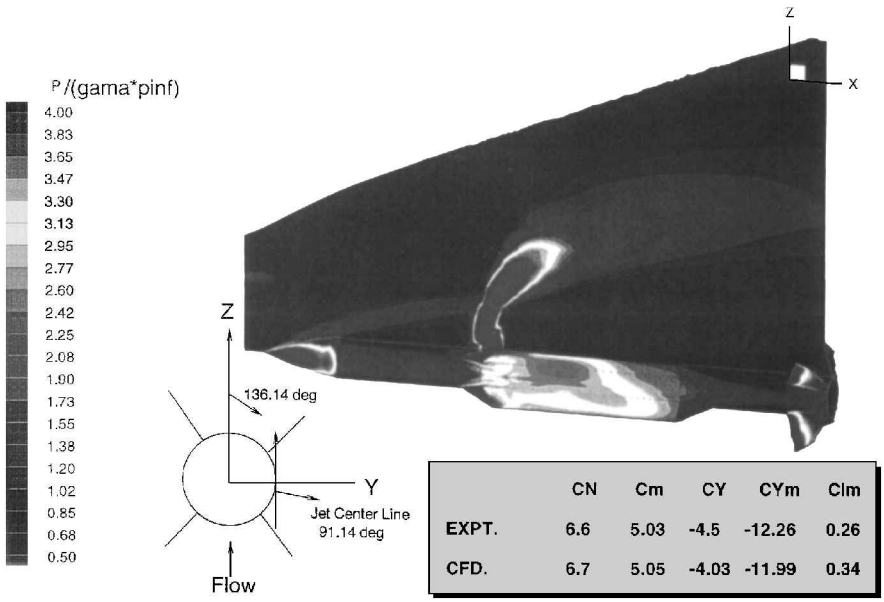

	CN	Cm	CY	CYm	Clm
EXPT.	6.6	5.03	-4.5	-12.26	0.26
CFD.	6.7	5.05	-4.03	-11.99	0.34

Fig. 4 Pressure distribution on jet center plane and missile surfaces for a side jet. Flow conditions: $M = 3.94$, $\alpha = 20$ deg, $\phi = 136.14$ deg, and jet thrust = 175 lb.

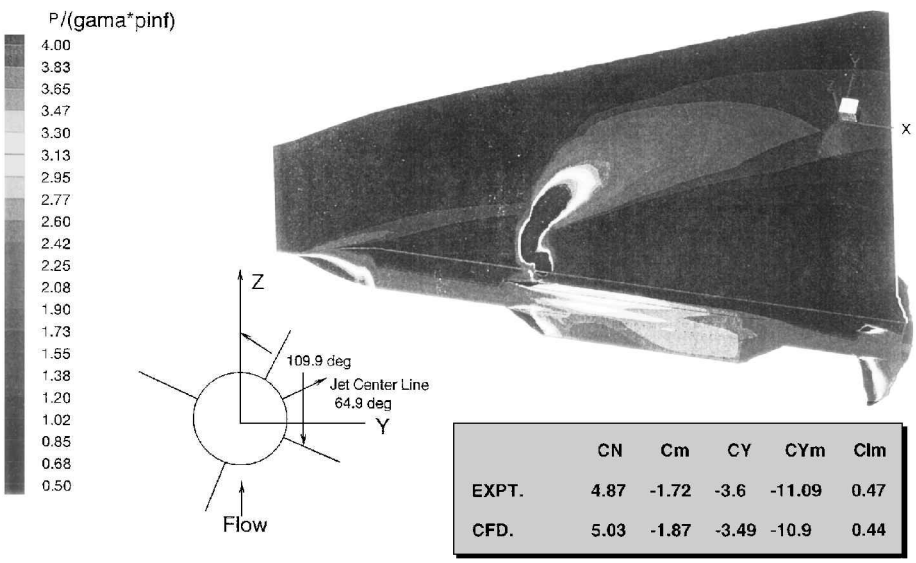

	CN	Cm	CY	CYm	Clm
EXPT.	4.87	-1.72	-3.6	-11.09	0.47
CFD.	5.03	-1.87	-3.49	-10.9	0.44

Fig. 5 Pressure distribution on jet center plane and missile surfaces for a leeward jet. Flow conditions: $M = 3.94$, $\alpha = 20$ deg, $\phi = 109.9$ deg, and jet thrust = 175 lb.

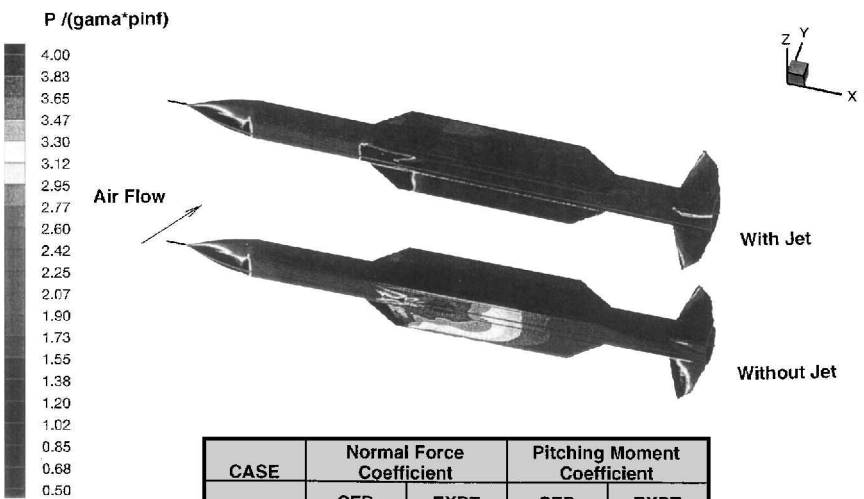

CASE	Normal Force Coefficient		Pitching Moment Coefficient	
	CFD	EXPT	CFD	EXPT
Jet On	8.96	8.71	22.56	22.5
Jet Off	7.3	6.8	5.96	5.97

Fig. 6 Pressure distribution showing jet interaction effects (forward missile body jet). Flow conditions: $M = 3.94$, $\alpha = 20$ deg, and jet thrust = 175 lb (total).

Fig. 7 Surface pressure distribution showing jet interaction effects (rear missile body jet). Flow conditions: $M = 3.94$, $\alpha = 20$ deg, and jet thrust = 175 lb (total).

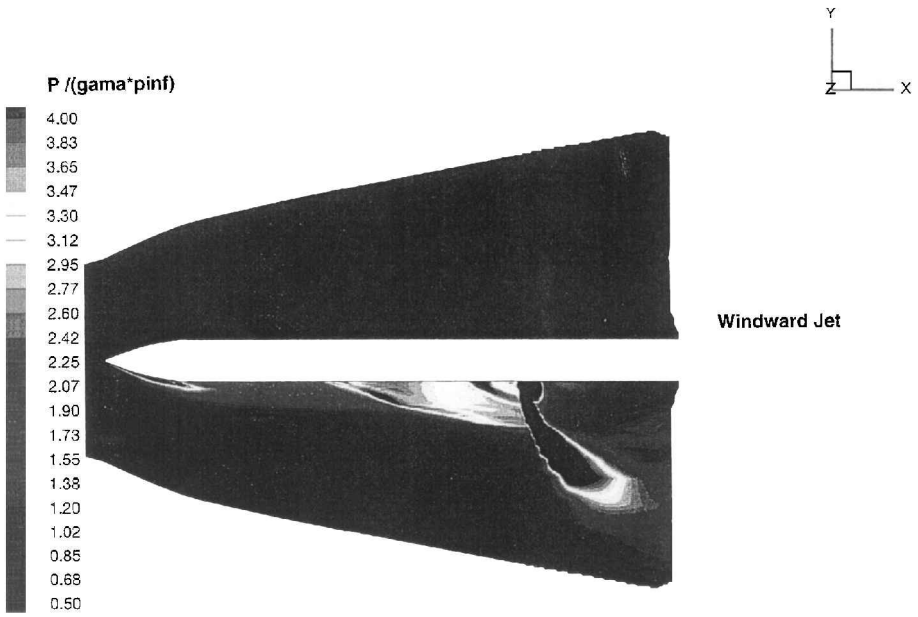

Fig. 8 Pressure distribution showing jet interaction effects for a rear missile body-mounted jet. Flow conditions: $M = 3.94$, $\alpha = 20$ deg, and jet thrust = 175 lb (total).

For these computed cases, the overall results are 1) jet thrust coefficient $(T/q \cdot S) = 3.45$, 2) total airframe only: normal force coefficient $CN_{\text{no-jet}} = 7.3$ and without-jet thrust $CN_{\text{jet}} = 5.51$, 3) normal force amplification factor $1 + [(CN_{\text{jet}} - CN_{\text{no-jet}})/\text{jet thrust coefficient}] = 0.48$, 4) tail normal force coefficient $(CN_{\text{tail}})_{\text{no-jet}} = 0.69$ and $(CN_{\text{tail}})_{\text{jet}} = 0.3$, and 5) tail effectiveness with jet $(CN_{\text{tail}})_{\text{jet}}/(CN_{\text{tail}})_{\text{no-jet}} = 0.43$.

Rear Jet

Figures 7 and 8 show the CFD computed pressure contours for the same geometry but with the jet thruster moved to the rear of the missile body; all other parameters were kept the same. Compare Fig. 7 with the jet-off case shown in the bottom of Fig. 6. Note that the rear part of the windward wings has developed substantially larger positive pressure due to the jet effects. Figure 8 shows the same result in the symmetry plane, highlighting the formation of a positive pressure zone ahead of the jet. The extent of this zone appears to be quite large because the jet does not encounter a head-on freestream at the rear but rather a low-momentum zone, and thus, the jet expands forward. This is a very favorable effect that will enhance the amplification factor. The amplification factor for this case is 1.056, a substantial increase in comparison to the value 0.48 for the forward body-mounted jet. However, note that the rear tail panels remain ineffective due to the jet blockage effect. For this case the aerodynamic results are 1) jet thrust coefficient = 3.42, 2) total airframe only: force coefficient with jet on = 7.49 (without jet thrust coefficient), 3) normal force amplification factor = 1.056, 4) tail normal force coefficient = 0.158, and 5) tail effectiveness with jet = 0.23.

Note that further loss of force coefficient on the tail has occurred for this jet location. This deficiency needs to be improved.

Figure 9 shows a summary of all of the preceding results highlighting the jet effectiveness for the two locations.

Wing Tip-Mounted Jet Thruster

Rectangular Slit Nozzle Cases

Forward jet. Jet thrusters exhausting from the wing tips are examined in this section. A narrow slit on the tip of the wing, which emulated the jet thruster, was created. Because the jet is now mounted on the wing, in an X orientation, symmetry dictates two jets. For this simulation the jet exit pressure ratio was maintained to be the same as in the preceding case, yielding a total jet thrust coefficient of 3.808.

Figure 10 shows the computational pressure contours indicating that the windward wing pressures are not lost; as well, the tail control power is retained for this case. For this case, the aerodynamic parameters are 1) jet thrust coefficient = 3.808, 2) total airframe only: normal force coefficient = 7.54 (without jet thrust coefficient),

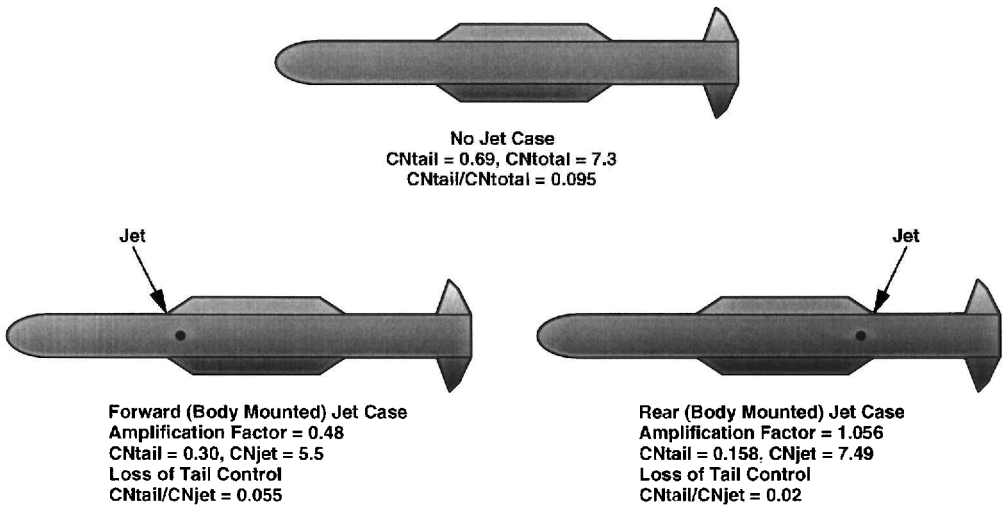

Fig. 9 Lateral jet thruster effectiveness studies for a missile with body-mounted jets. Flow conditions: $M = 3.94$ and $\alpha = 20$ deg (baseline dorsal, windward jet).

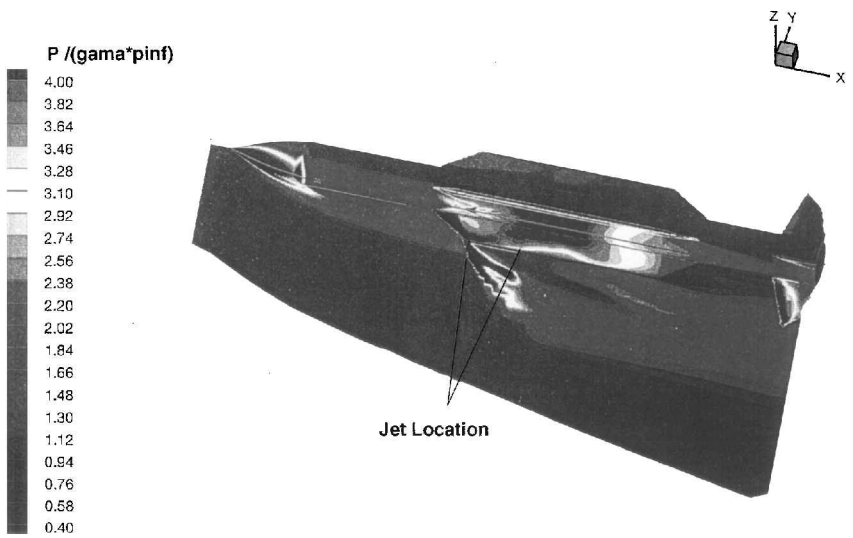

Fig. 10 Missile surface and windward wing plane pressure contours for a forward wing tip-mounted jet (narrow slit nozzle). Flow conditions: $M = 3.94$, $\alpha = 20$ deg, and jet thrust = 97 lb (each wing).

3) force amplification factor = 1.064, 4) tail normal force coefficient = 0.603, and 5) tail effectiveness with jet = 0.87.

Note that the tail CN for this case is almost fully recovered to the jet-off case, as shown in Fig. 6.

Rear jet. Figure 11 shows a computation for where the jet was moved to the rear of the wing. Note from Fig. 11 that the flow details are markedly different as compared to the forward tip-mounted jet shown in Fig. 10. For this case the aerodynamic results are 1) jet thrust coefficient = 3.54, 2) total airframe only: normal force coefficient = 7.5 (without jet thrust coefficient), 3) force amplification factor = 1.057, 4) tail normal force coefficient = 0.74, and 5) tail effectiveness with jet = 1.073.

Note from these results that the tail panels have fully recovered the control power. This case, then, appears to be most satisfactory.

Figure 12 shows the results for the wing tip-mounted jets. Comparing all of the results shown, it appears that the wing tip-mounted jet will yield the desired goals for this missile frame.

A somewhat more detailed comparison of the two wing tip-mounted jets is shown in Fig. 13. Figure 13 shows the pressure differential between the jet-on and jet-off conditions for the two cases. Notice from Fig. 13 that the positive effects are more prominent in the tail area for the rear wing tip-mounted jet.

Rolled wings. In an effort to address the question of whether the rear wing-mounted jets are as effective in different missile orientations, we have studied a case with a plus missile orientation. The thrust ratio for this missile orientation was 1.76. This level was chosen to ensure symmetry in CFD calculations without changing the missile wing geometry. This is achieved by keeping the thrust level from the windward wing the same as in the last computation. Qualitative comparisons with earlier cases can still be made. All other flow conditions were maintained the same as in the other cases. For this case the aerodynamic results are 1) jet thrust coefficient = 1.76, 2) total airframe only: normal force coefficient = 7.33 (jet off) and 7.21 (jet on), 3) force amplification factor = 0.93, 4) tail normal force coefficient = 0.63 (jet off) and 0.56 (jet on), and 5) tail effectiveness with jet = 0.89.

Thick Wing Nozzle Cases

As discussed before, the structural, packaging, and other engineering issues associated with the narrow slit nozzle on wing tips present challenging requirements for the overall missile design. Computational results with diamond-shaped chordwise cross sections, to study the effect of square nozzles, are presented next.

Forward jet. The missile geometry with forward wing tip nozzle was used to study the forward wing tip-mounted divert jet. The study was performed in an X orientation with two forward wing tip-mounted jets (on the windward side) yielding 108 lb of thrust from each wing tip nozzle. The results for this CFD simulation are shown in Figs. 14 and 15. Figure 14 shows the computed pressure distribution on the missile surfaces and a plane containing the jet (looking at it from the windward side). Note from Fig. 14 that the forward wing tip-mounted jet creates favorable pressures on the

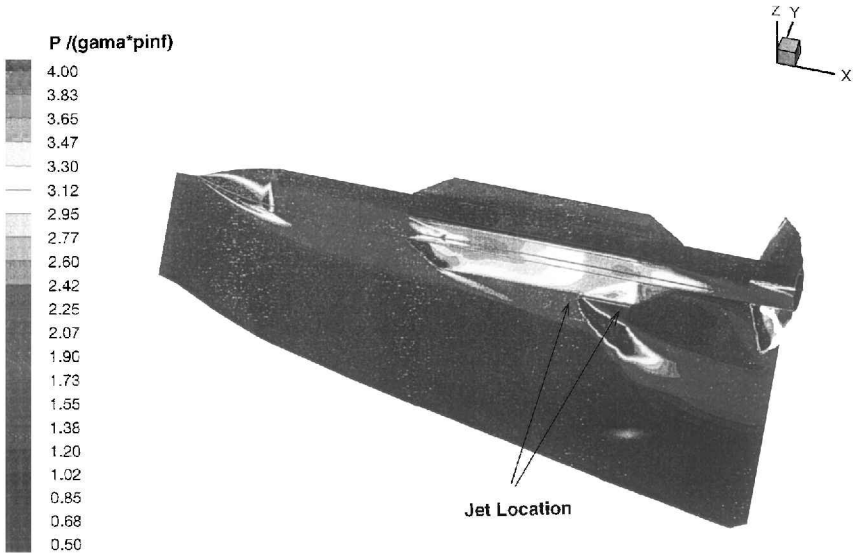

Fig. 11 Missile surface and windward wing plane pressure contours for a wing tip-mounted jet (narrow slit nozzle). Flow conditions: $M = 3.94$, $\alpha = 20$ deg, and jet thrust = 90 lb (each wing).

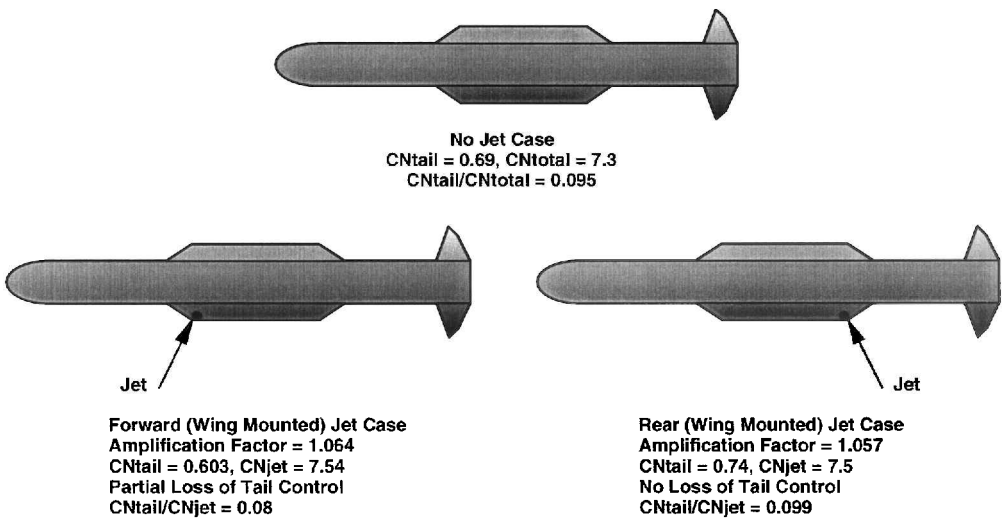

Fig. 12 Lateral jet thruster effectiveness studies for a missile with wing tip-mounted jets (narrow slit). Flow conditions: $M = 3.94$ and $\alpha = 20$ deg (baseline dorsal, windward jet).

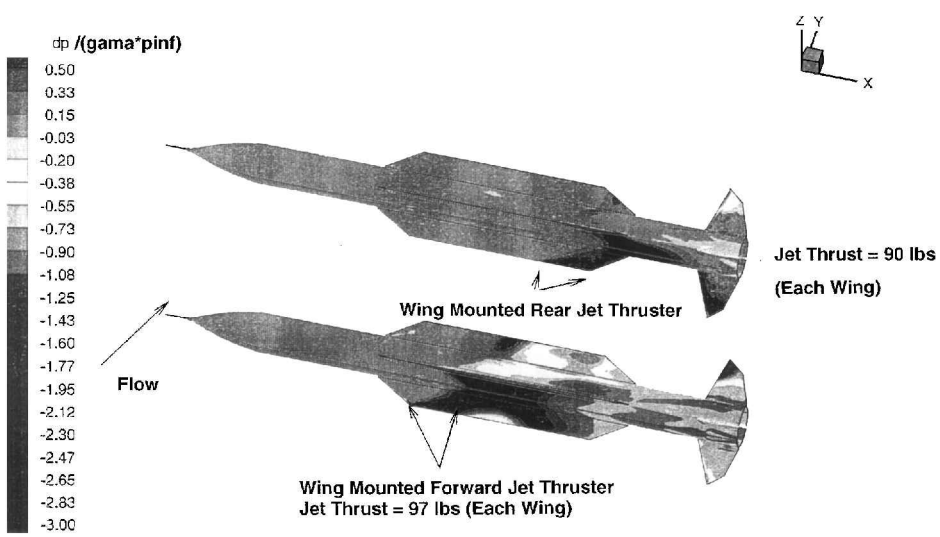

Fig. 13 Pressure differential for jet on and jet off showing jet interaction effects for wing tip-mounted jets (narrow slit nozzle). Flow conditions: $M = 3.94$ and $\alpha = 20$ deg.

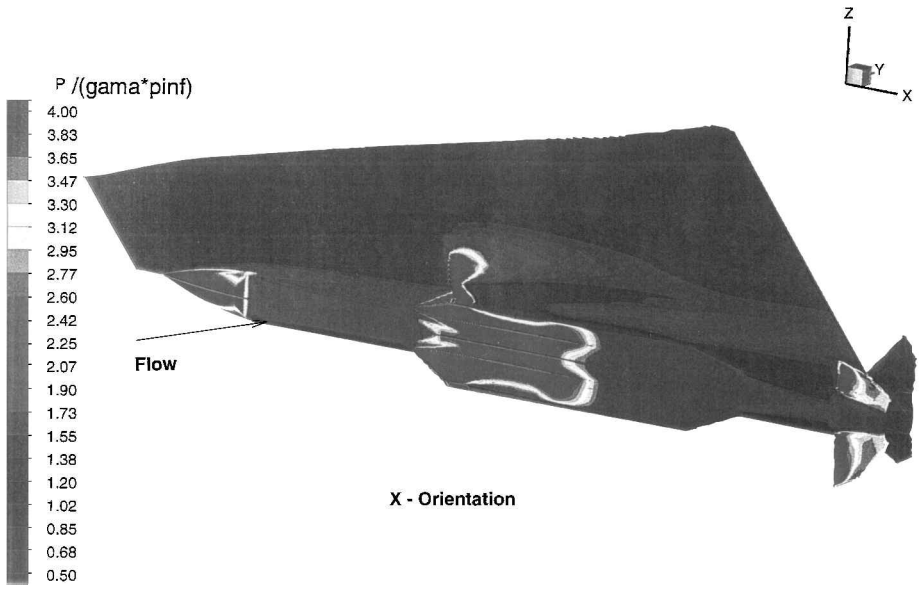

Fig. 14 Pressure distribution for missile surfaces and a plane containing the jet for a forward thick wing tip-mounted jet (square nozzle). Flow conditions: $M = 3.94, \alpha = 20$ deg, and jet thrust = 108 lb (each wing).

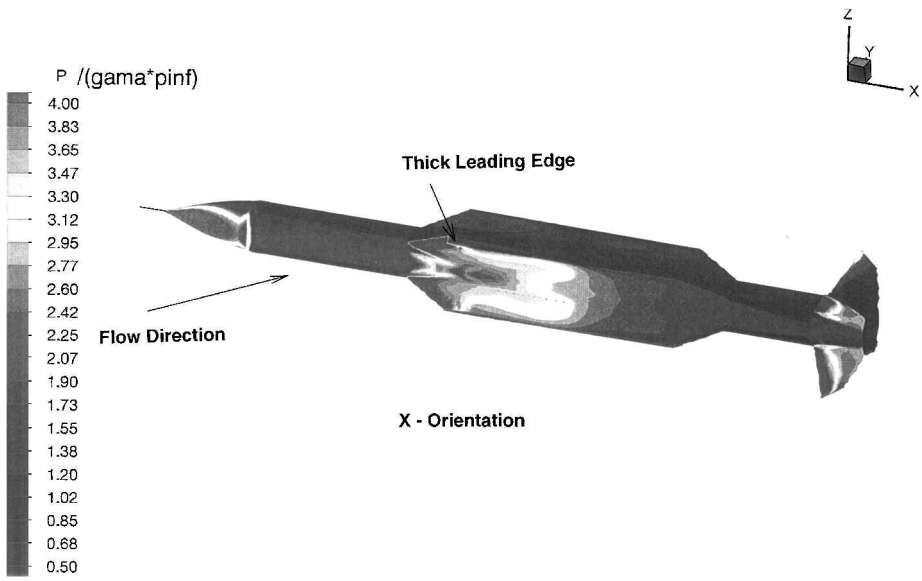

Fig. 15 Pressure distribution on missile surfaces for a forward thick wing without jet. Flow conditions: $M = 3.94$ and $\alpha = 20$ deg (no-jet case).

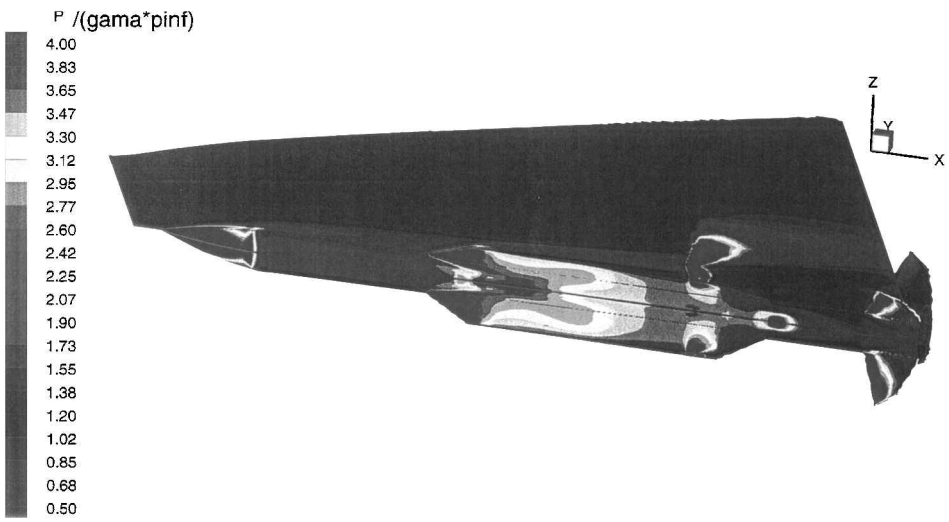

Fig. 16 Pressure distribution on missile surfaces and a plane containing divert jet for a rear thick wing tip-mounted jet (square nozzle). Flow conditions: $M = 3.94, \alpha = 20$ deg, and jet thrust = 108 lb (each wing).

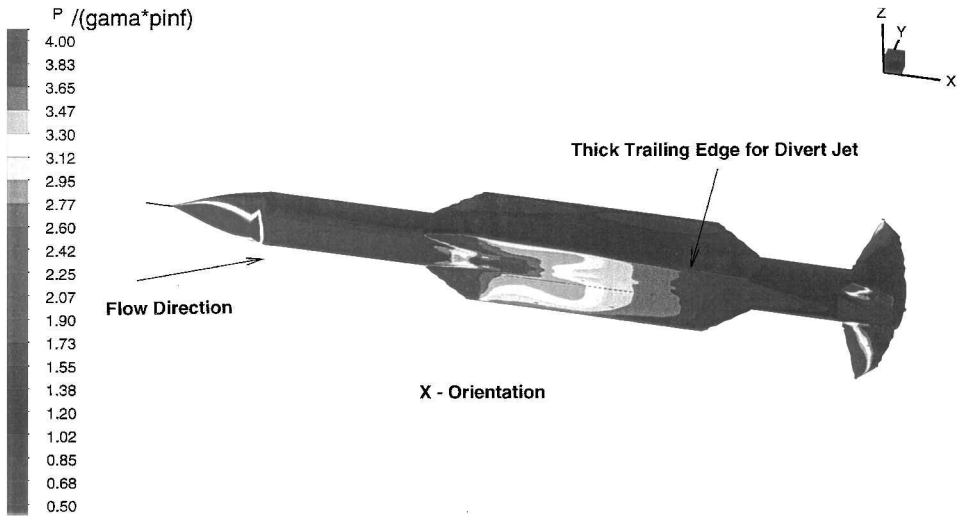

Fig. 17 Pressure distribution on missile surfaces without rear wing tip-mounted divert jet. Flow conditions: $M = 3.94$ and $\alpha = 20$ deg.

windward wings and the tails. This is apparent if one compares the jet-on case in Fig. 14 with the jet-off case in Fig. 15. The overall results for the two computations are 1) jet thrust coefficient = 4.25, 2) total airframe only: normal force coefficient = 6.94 (jet on) and without jet thrust coefficient = 6.61 (jet off), 3) normal force amplification factor = 1.076, 4) tail normal force coefficient = 0.65 (jet on) and 0.67 (jet off), and 5) tail effectiveness with jet = 0.97.

These computational results show that a forward wing tip-mounted thick wing nozzle case gives a high normal force amplification factor, as well as retaining the tail effectiveness.

Rear jet. The missile geometry with rear wing tip nozzle was used to study the rear wing tip-mounted divert jet. Figures 16 and 17 show the results with and without jet, respectively. Note from Fig. 16 that the rear wing tip-mounted jet creates a missile surface pressure distribution that is quite distinct from that seen in Fig. 14, with forward wing tip jet. Figure 17 shows a corresponding jet-off case. The overall computational results for the two cases are 1) jet thrust coefficient = 4.25, 2) total airframe only: normal force coefficient = 7.05 (jet on) and without jet thrust coefficient = 6.77 (jet off), 3) normal force amplification factor = 1.066, 4) tail normal force coefficient = 0.73 (jet on) and 0.68 (jet off), and 5) tail effectiveness with jet = 1.074.

Overall results show that the wing tip-mounted divert thruster, forward or rear, gives higher normal force amplification factors than the missile body-mounted divert thrusters. Additionally, the former do not interfere with the missile tail effectiveness. A forward wing tip-mounted divert jet will also yield a very high positive (desirable) pitching moment amplification as compared to the rear wing-tip mounted jet. Utilization of the forward wing tip-mounted divert jet is recommended to improve the aerodynamic performance and maneuverability for future missile systems.

Conclusions

Computational results were presented to show that aerodynamic force and moment coefficients for asymmetric missile configurations with divert jet can be predicted well in comparison to the wind-tunnel data. Subsequent computations show that the loss of the amplification factor for a windward-oriented jet can be recovered by appropriately selecting the jet location. Specifically, it has been shown that a jet thruster mounted on the wing tip eliminates all undesirable effects, yielding a high amplification factor, as well as retaining the tail control power.

References

[1]Cassel, L. A., Davis, J. G., and Engh, D. P., "Lateral Jet Control Effectiveness Prediction for Axisymmetric Missile Configurations," U.S. Army Missile Command, Rept. RD-TR-68-5, Redstone Arsenal, AL, June 1968.

[2]Spring, D., "An Experimental Investigation of the Interference Effects Due to a Lateral Jet Issuing from a Body of Revolution over the Mach No. Range of 0.8 to 4.5," U.S. Army Missile Command, Rept. RD-TR-68-10, Redstone Arsenal, AL, Aug. 1968.

[3]Srivastava, B., "Computational Analysis and Validation for Lateral Jet Controlled Missiles," *Journal of Spacecrafts and Rockets*, Vol. 34, No. 5, 1997, pp. 584–592; also AIAA Paper 96-0288, Jan. 1996.

[4]Srivastava, B. N., "Lateral Jet Control of a Supersonic Missile: CFD Predictions and Comparisons to Force and Moment Measurements," AIAA Paper 97-0639, Jan. 1997.

[5]Chamberlain, R., "Control Jet Interaction Flowfield Analysis," *Aerodynamic Investigations*, Lockheed Rept. LMSC F268936, Vol. 5, Feb. 1990.

[6]Chamberlain, R., "Calculation of Three-Dimensional Jet-Interaction Flowfields," AIAA Paper 90-2099, 1990.

[7]Weatherly, D., and McDonough, J., "Performance Comparisons of Navier–Stokes Codes for Simulating Three-Dimensional Hypersonic Crossflow/Jet Interaction," AIAA Paper 91-2096, 1991.

[8]York, B. J., Sinha, N., Kenzakowski, D. C., and Dash, S. M., "PARCH Code Simulation of Tactical Missile Plume/Airframe/Launch Interactions," *19th JANNAF Exhaust Plume Technology Meeting*, CPIA PWB 568, Chemical Propulsion Information Agency, Laurel, MD, 1991, pp. 645–674.

[9]Chan, S. C., Roger, R. P., Edwards, G. L., and Brooks, W. B., "Integrated Jet Interactions CFD Predictions and Comparison to Force and Moment Measurements for a Thruster Attitude Controlled Supersonic Missile," AIAA Paper 93-3522, 1993.

[10]Lytle, J. K., Harloff, G. J., and Hsu, A. T., "Three-Dimensional Compressible Jet-in-Crossflow Calculations Using Improved Viscosity Models and Adapted Grid," AIAA Paper 90-2100, 1990.

[11]Dash, S. M., Sinha, N., York, B. J., Lee, R. A., and Hosangadi, A., "On the Inclusion of Advanced Turbulence Models and Nonequilibrium Thermochemistry into State-of-the-Art CFD Codes and Their Validation," AIAA Paper 92-2764, 1992.

[12]Rizzetta, D. P., "Numerical Simulation of Slot Injection into a Turbulent Supersonic Stream," AIAA Paper 92-0827, 1992.

[13]Darmieux, M., and Marasaa-Poey, R., "Numerical Assessment of Aerodynamic Interactions on Missiles with Transverse Jets Control," *AGARD Meeting on Computational and Experimental Assessment of Jets in Cross Flow*, 1993.

[14]Dash, S. M., York, B. J., Sinha, N., Lee, R. A., Hosangadi, A., and Kenzakowski, D. C., "Recent Developments in the Simulation of Steady and Transient Transverse Jet Interactions for Missile, Rotorcraft, and Propulsive Applications," *AGARD Meeting on Computational and Experimental Assessment of Jets in Cross Flow*, 1993.

[15]Chan, S. C., Roger, R. P., Brooks, W. B., Edwards, G. L., and Boukather, S. B., "CFD Predictions and Comparisons to Wind Tunnel Data for the Asymmetric Firing of a Forward Mounted Attitude Control Thruster," AIAA Paper 95-1895, June 1995.

[16]Qin, N., and Foster, G. W., "Study of Flow Interactions Due to a Supersonic Lateral Jet Using High Resolution Navier–Stokes Solutions," AIAA Paper 94-2151, June 1994.

[17]Steinbrenner, J. P., and Chawner, J. R., "Recent Enhancements to the GRIDGEN Structural Grid Generation System," *Proceedings of the NASA Workshop on Software Systems for Surface Modeling and Grid Generation*, Hampton, VA, 1992.

E. V. Zoby
Editor-in-Chief